Journal of Theoretical and Computational Chemistry
Vol. 9, No. 4 (2010) 797–812

DOI: 10.1142/S0219633610005980

World Scientific
www.worldscientific.com

STUDY ON THE INTERACTIONS OF Smac MIMETICS WITH XIAP-BIR3 DOMAIN BY DOCKING AND MOLECULAR DYNAMICS SIMULATIONS

BAOPING LING*, RUI ZHANG†, ZHIGUO WANG†,
YONGJUN LIU*,†,‡ and CHENGBU LIU*

*School of Chemistry and Chemical Engineering
Shandong University, Jinan, Shandong 250100, P. R. China

†Northwest Institute of Plateau Biology
Chinese Academy of Sciences, Xining, Qinghai 810001, P. R. China
* yongjunliu_1@sdu.edu.cn

Received 15 January 2010
Accepted 30 March 2010

Upon receiving an apoptotic stimulus, the mature mitochondrial protein second mitochondria-derived activator of caspases (Smac)/direct IAP-binding protein with low PI (DIABLO), which could be released from mitochondria into the cytosol together with cytochrome C, specifically binds to inhibitor of apoptosis proteins (IAPs) and relieves the inhibitory effect of caspase, thus promotes cell death. Some artificial small molecules (called Smac mimetics) can mimic the *N*-terminal four residues Ala1-Val2-Pro3-Ile4 (AVPI) sequence of mitochondrial protein Smac, and competitively bind to X-linked inhibitor of apoptosis protein baculoviral IAP repeats (XIAP-BIR3) domain with caspase-9, which leads to the removal of the inhibition of caspase-9 by XIAP and induce apoptosis. To gain an insight into the nature of XIAP-BIR3 domain recognizing Smac mimetics, we used docking and molecular dynamics simulations methods to study four representative Smac mimetics. The docking results show that the orientations of these backbones of ligands are identical with that of AVPI in the binding pocket. Each ligand corresponds to two competitive conformations, which are called extended and bended conformations. The results of molecular dynamics simulations show that the extended conformation is more stable, and the calculations of energy decomposition reveal that the residue Thr308 makes the strongest interaction with XIAP-BIR3. In addition, Asp309, Glu314, and Trp323 are indispensable for XIAP-BIR3 recognizing and binding Smac mimetics.

Keywords: Inhibitor of apoptosis protein (IAP); Smac mimetics; molecular docking; molecular dynamics simulations; binding free energy.

1. Introduction

Apoptosis, also called programmed cell death, is an essential process in the development and homeostasis of the multicellular organisms.[1,2] Malignant disorders of

‡Corresponding author.

apoptotic process could lead to a number of diseases directly or indirectly, such as cancer and Alzheimer's disease.

Inhibitor of apoptosis protein (IAP) is an endogenous antagonist of regulator caspase, which is a family of cysteine proteases that cleave their substrates after an aspartate or glutamate residue. The IAPs antagonize cell death by inhibiting the enzymatic activity of mature caspases.[3] The X-linked inhibitor of apoptosis protein (XIAP) is one member of the IAP family, and contains three baculoviral IAP repeats (BIR) domains and one zinc-binding BIR domain, each domain controlling a distinct function,[4–6] the third BIR domain (BIR3) can bind directly and inhibit potently the activity of caspase-9.[7,8]

The second mitochondria-derived activator of caspases (Smac),[9] also known as direct IAP-binding protein with low pI (DIABLO),[10] is a mitochondrial protein that antagonizes or counteracts one or more members of the IAP family and promotes apoptosis. Upon apoptotic stimuli, the mature Smac together with cytochrome C is released from the intermembrane space of mitochondria into the cytoplasm, and competes with caspase-9 for binding to the common residues of the surface groove in XIAP-BIR3 domain. Accordingly, this mechanism relieves caspase-9 inhibition by XIAP and promotes apoptosis.[11,12]

To date, two types of Smac mimetics, namely monovalent and bivalent, have been reported.[13] The monovalent compounds are designed to mimic the single Ala1-Val2-Pro3-Ile4 (AVPI) tetrapeptide sequence of Smac *N*-terminus,[14–16] whereas the divalent ones contain two AVPI sequences tethered together through a linker.[17,18] Although the divalent mimetics are of much higher affinities and more potent than their corresponding monovalent compounds in inducing apoptosis, the monovalent compounds with small molecular weight achieve more potential oral bioavailability. According to the structure of Smac bound to XIAP-BIR3 domain, a number of research groups have designed and synthesized a series of peptide and non-peptide Smac mimetics to mimic the tetrapeptide AVPI sequence in recent years.[19–23] However, these compounds are not suitable drug candidates because of their limitation of cellular activity and poor stability *in vivo*; hence, many groups pursue a new class of anticancer drugs.

On the basis of *N*-terminal AVPI tetrapeptide sequence of natural endogenous inhibitor Smac of IAPs, the Wang's group[17,21,24–28] reported a series of conformationally constrained monovalent and divalent non-peptide Smac mimetics. They found that bicyclic core Smac mimetics with seven-member rings, which were cyclized by the isopropyl group of Val2 and the five-membered ring of Pro3, were highly potent.[29] Oost *et al.*[30] revealed that the methylated free amino group contributed to improve the cellular activity of mimetics. Accordingly, based on the backbones of these cyclized Smac mimetics with seven-member rings, Sun *et al.*[31] methylated the primary amino group to enhance their cell permeability. The slight change was made on the free amino group, but the cellular activity and permeability were remarkably different. For example, when the amino-terminus of Smac mimetics was replaced by primary amino group or methylated secondary amino group,

the corresponding inhibition constants K_i were 65 and 21 nM, and the values of IC_{50} were 50 and 0.1 μM, respectively. When the substituent was tertiary amino group, K_i dramatically decreased to 14.4 μM while the IC_{50} value of 3.0 μM had no obvious change.[31] The reason that caused the values of K_i and IC_{50} to change significantly is unclear. At present, most studies have focused on the development of new Smac mimetics, but comparatively little research has examined the issue of theory. The calculating method of the binding free energy of XIAP-BIR3 complexing with Smac mimetics had been provided.[32−35] However, the structural change effect on the binding mode and affinity are unclear to date.

To better understand how Smac mimetics bind to XIAP-BIR3 domain and reduce inhibition of caspases-9, on the basis of Sun's experiment,[31] we used docking and molecular dynamics (MD) simulations methods to investigate four monovalent Smac mimetics with different substituents, and analyzed the binding mode and affinity in detail. We also employed the molecular mechanics Poisson–Boltzmann surface area (MM-PBSA) method to calculate the binding free energy, and performed energy decomposition to study the contribution of each residue. These studies help us to understand the mechanism of apoptosis induction in a cell.

2. Computational Details

Wang's group[31] has designed and synthesized a series of Smac mimetics, and studied their binding mode and inhibition activity. Based on these experimental results, we carried out molecular docking and MD simulations to investigate the interactions of four representative Smac mimetics with XIAP-BIR3. The XIAP-BIR3 model was obtained from Brookhaven Protein Data Bank (www.rcsb.org). The ID code is 1G73 with a resolution of 2.0 Å. The crystal structure was a dimeric polymer, so we selected chain C to serve as the receptor and retained zinc ion to stabilize XIAP-BIR3 domain, as shown in Fig. 1. Before docking, all substances except the receptor were removed from the crystal structure. Then, AutoDock 4.0 program[36] was applied to add polar hydrogen atoms and assign Kollman united atom partial charge to the receptor. The chemical structures of the four bicyclic core Smac mimetics were shown in Fig. 2, and their spatial conformations were optimized using Gaussian 03 program[37] at the B3LYP/6-31G level.

2.1. *Parameters' setup for docking*

The docking calculations were performed with the AutoDock 4.0 package, which was based on the Lamarck genic algorithm and empirical free energy function.[36] The center of the grid box was set to the residue Leu307, the size of box was set to $60 \times 60 \times 60$ points with grid spacing of 0.375 Å, which was large enough for the free rotation of the ligand. When docking, the maximum number of energy evaluations was set to 2.5×10^7, the rest of docking parameters were set to default values. As many as 50 independent docking experiments were run for each ligand, the docking conformations were clustered according to the criterion of 2.0 Å root-mean-square

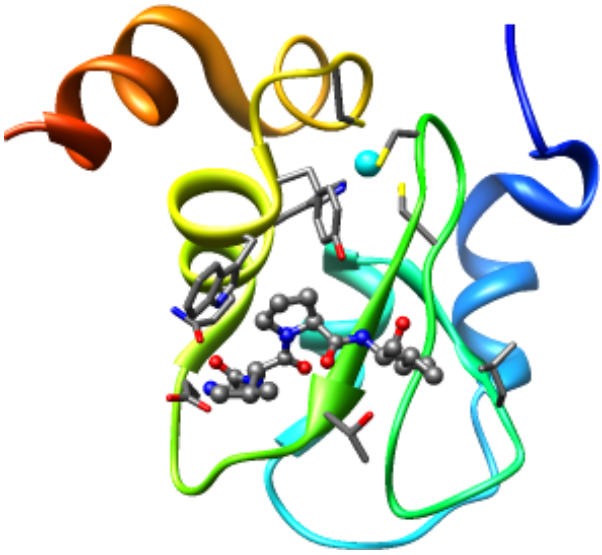

Fig. 1. Three-dimensional structure of XIAP-BIR3 domain bound to Smac *N*-terminal tetrapeptide AVPI which is shown in ball and stick (PDB code: 1G73). The zinc atom is colored by cyan and shown by the round objects. Color online.

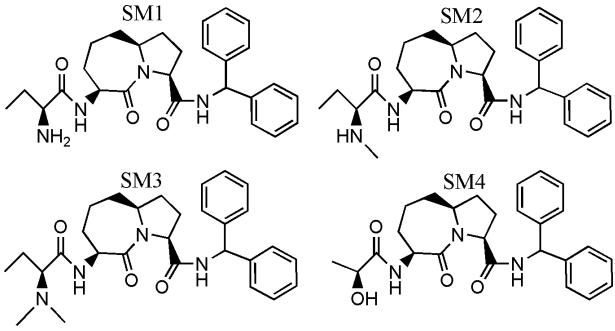

Fig. 2. Chemical structures of the bicyclic core Smac mimetics.

deviation (RMSD), and the two preferred conformations were selected as the initial structures for MD simulations.[38]

2.2. *Parameters' setup for MD simulations*

The docking conformation was solvated in a $56.2 \times 56.2 \times 56.2$ Å TIP3P water box with periodic boundary conditions; then, two sodium counterions were added to maintain the system neutralization. All the MD simulations were performed in Amber99[39] force field in an NPT ensemble. Long-range electrostatic interaction was treated by using particle mesh Ewald (PME) method with a cutoff of 9 Å.

The SHAKE algorithm was employed to constrain all bonds involving hydrogen bonds. Langevin dynamics was employed to control the temperature at 300 K using a collision frequency of 1.0 ps^{-1}, and isotropic position scaling was used to maintain the pressure of 1.0 atm with a relaxation time of 2 ps.[40] The cationic dummy atoms method was used to treat the zinc ion of XIAP-BIR3 domain, this method was successfully applied to the calculations of matrix metalloproteinase[41] and phosphotriesterase.[42]

At first, we used a harmonic distance constraint with a force constant of 500 kcal/(mol·Å^2) to restrain the protein, ligand, and cationic dummy atoms, and the conjugate gradient and steepest descent method were used to minimize the system energy. Subsequently, the whole system was allowed to move to release the steric collision from the starting structure. Second, the position-restrained MD was carried out to equilibrate the water molecules for 250 ps, with a force constant of 10 kcal/(mol·Å^2) to fix the protein and ligand. Finally, 5 ns MD simulations were calculated for the whole system after all restraints were removed, the time step was set to 2 fs and the MD trajectories were saved every 2 ps.[40]

2.3. *Parameters' setup for the binding free energy and energy decomposition*

The MM-PBSA method[43] has been successfully employed in calculating the binding free energies of a number of protein systems.[44,45] We extracted 50 snapshots from an MD trajectory to calculate the average binding free energy of the system. Normal mode calculation was extremely time consuming and computationally expensive; therefore, we extracted 10 snapshots from an MD trajectory to calculate the entropy contribution. The MM-PBSA method was used to decompose energy into individual contributions for all residues of the receptor. During the calculation, the dielectric constants for solvent and solute were set to 80.0 and 1.0, respectively. Solvent probe radius was 1.4 Å and the maximum number of cycles was 1000 steps.[46] According to the MM-PBSA method, the binding free energy could be described as follows[47]

$$\Delta G_{\text{bind}} = G_{\text{complex}} - (G_{\text{receptor}} + G_{\text{ligand}}) \tag{1}$$

$$\Delta G = \Delta E_{\text{MM}} + \Delta G_{\text{solv}} - T\Delta S \tag{2}$$

In which

$$\Delta E_{\text{MM}} = \Delta E_{\text{int}} + \Delta E_{\text{ele}} + \Delta E_{\text{vdw}} \tag{3}$$

$$\Delta G_{\text{solv}} = \Delta G_{\text{PB}} + \Delta G_{\text{SA}} \tag{4}$$

$$\Delta G_{\text{SA}} = \gamma \text{SA} + b \tag{5}$$

where in ΔG_{bind} accounts for the binding free energy, G_{complex}, G_{receptor}, and G_{ligand} represent the free energies for complex, receptor, and ligand, respectively. ΔE_{MM} is calculated by averaging the energies of molecular mechanics in vacuum, and composed of internal energy (ΔE_{int}), electrostatic energy (ΔE_{ele}), and van der

Waals (ΔE_{vdw}) interactions. Solvation free energy (ΔG_{solv}) is decomposed into polar solvation free energy (ΔG_{PB}) evaluated using the Poisson–Boltzmann equation, and non-polar solvation free energy (ΔG_{SA}) from the solvent accessible surface area determined with the LCPO model, γ and b are 0.00542 kcal/(mol·Å^2) and 0.92 kcal/mol, respectively. T is absolute temperature and ΔS is entropy term obtained by normal mode analysis.

3. Results and Discussions

3.1. *Molecular docking*

The crystal structures revealed that Smac recognized a surface groove on the BIR3 domain through N-terminal tetrapeptide AVPI sequence which established a network of hydrogen bonds, electrostatic contacts, van der Waals, and hydrophobic interactions with neighboring residues of XIAP-BIR3.[15,16] Ala1 played an important role in specific recognition. Besides forming hydrogen bonds with Glu314, it established hydrophobic and electrostatic interactions with the surrounding residues, and affected the binding affinity of complex.[16]

The docking conformations of four bicyclic core Smac mimetics are shown in Fig. 3. The docking results show that these ligands can be docked into the surface groove of XIAP-BIR3 domain, and each ligand exhibits two competitive conformations in the binding pocket. The conformation with the lowest energy is defined as *a* form, whereas the higher is *b* form. Various energies obtained from the docking are listed in Table 1.

The two docking conformations of SM1, namely SM1_a and SM1_b, are given in Fig. 3(a). SM1_a forms four hydrogen bonds with BIR3 domain, two of which are formed between the free amino group and Glu314, and the others are generated between the nitrogen atom in amide group and oxygen atom in lactam and Trp308, respectively. While SM1_b forms five hydrogen bonds with BIR3, those between amide and lactam or Trp308 are the same as those in SM1_a. However, free amino group forms one hydrogen bond with Glu314 and Gln309, respectively. In addition, the carbonyl in amide interacts with Trp323 to form one hydrogen bond.

The bicyclic core segments in SM1_a and SM1_b parallel to the indole ring of Trp323. The differences between SM1_a and SM1_b are that the ethyl of amino-terminus in SM1_a is located in the hydrophobic pocket composed of side chains of Leu307 and Trp310, closing to the indole ring of Trp310, while the ethyl in SM1_b oppositely extends into the solvent. The free amino group is protonated under physiological conditions, when it closes to Glu314, the electrostatic interaction between SM1_a and Glu314 is enhanced, whereas the free amino group of SM1_b is far away from Glu314. In addition, the terminal diphenylmethyl of two conformations have different orientations. Although the number of hydrogen bonds of SM1_b is larger than that of SM1_a, the electrostatic and van der Waals interactions of SM1_b are weaker than those of SM1_a (Table 1), so SM1_a corresponds

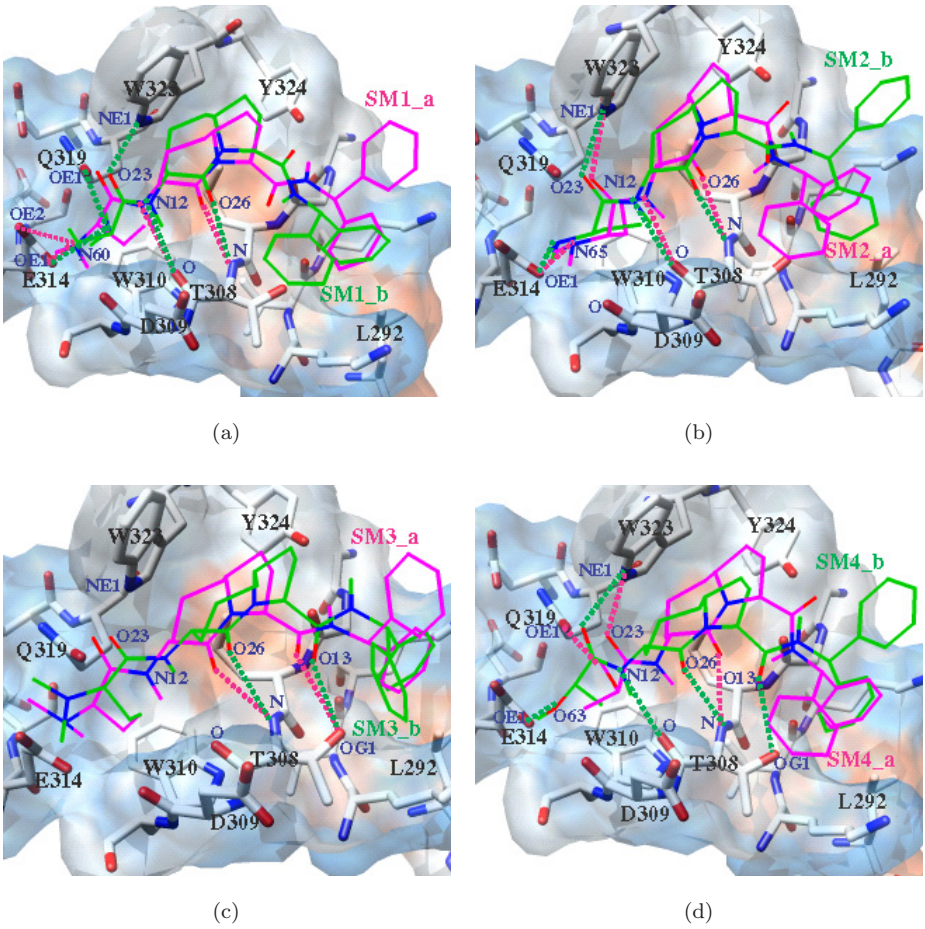

Fig. 3. The docking structures of the bicyclic cores of Smac mimetics in complex with XIAP-BIR3 domain. Carbon atoms are shown in dim gray, oxygen and nitrogen atoms in red and blue, respectively. Hydrogen bonds are represented by dashed lines. The docking structure with the lowest energy is shown in magenta; and the second conformation with higher energy is shown in green. The hydrophobic surface shows the hydrophobicity of amino acid with colors ranging from dodger blue for the most hydrophilic to white at 0.0 to orange red for the most hydrophobic. Color online.

to the lower docking energy, and its binding modes and orientation are consistent with the crystal structures.[27,48,49]

The two conformations of SM2 correspond to the identical hydrogen bonding modes (Fig. 3(b)). Because of the steric hindrance of methyl, only one hydrogen bond is formed between nitrogen of methylated amino group and Glu314, but the oxygen atom of amide forms another hydrogen bond with the nitrogen atom of indole ring of Trp323. The other two hydrogen bonds of SM2 are the same as those of SM1. But for the orientations of diphenylmethyls, SM2_a is similar to SM1_b and

Table 1. Various energies (kcal/mol) of Smac mimetics binding to XIAP-BIR3 by docking.

Smac mimetics	Vdw+Hbond+ desolvation	Electrostatic energy	Binding energy	Experimental[a] $IC_{50,exp}(\mu M)$
SM1_a	−10.31	−2.05	−10.24	50
SM1_b	−10.06	−1.73	−9.97	
SM2_a	−10.74	−1.67	−11.21	0.1
SM2_b	−10.18	−1.84	−10.20	
SM3_a	−9.42	−0.97	−11.01	3.0
SM3_b	−9.13	−1.03	−9.87	
SM4_a	−10.09	−0.19	−9.31	70
SM4_b	−9.73	−0.43	−8.46	

[a]The experimental data are from Ref. 31.

SM2_b similar to SM1_a. Both for the two conformations of SM1 and SM2, only one phenyl is in the hydrophobic pocket.

Figure 3(c) shows the docking conformations of SM3. It can be seen that the hydrogen bonding modes of SM3_a and SM3_b are same, in which carbonyl of lactam and terminal amide form hydrogen bonds with Thr308. Because of the steric hindrance, no hydrogen bond was formed between the methylated amino group and Glu314. The terminal diphenylmethyl orientates differently and one phenyl is overlapped in the two conformations.

The docking conformations of SM4 are shown in Fig. 3(d). SM4 also corresponds to two conformations, but the number and binding mode of hydrogen bonds change slightly compared with those of other ligands.

In summary, each Smac mimetic exhibits two favorite conformations on the surface groove of XIAP-BIR3. Although their binding modes are slightly different, the bicyclic core segments always parallel to the indole ring of Trp323, the amino-terminal amide and lactam form strong hydrogen bonding interactions with Thr308, which is important for ligand bound to XIAP-BIR3. The docking energies in Table 1 show that the electrostatic interaction is weakened with the amino group methylated. When the free amino group bears one methyl (SM2), the sum of van der Waals, hydrogen bond and desolvation energy is the biggest, and the binding energy of SM2_a is the lowest, which is in agreement with the experimental result.[31]

Figure 4 shows the superimpositions of extended and bended conformations of four ligands on the surface of XIAP-BIR3. One can see that four ligands are superimposed with the backbone of AVPI sequence. Only in the extended conformations, the orientation of phenyl matches well with that of Ile4. The crystal structures resolved by Sun *et al.* and Mastrangelo *et al.* proved that Smac mimetics adopted extended conformations on the surface groove of XIAP-BIR3.[27,48,49] The docking results show us two competitive conformations, therefore we performed MD simulations to explore the stability of the conformations.

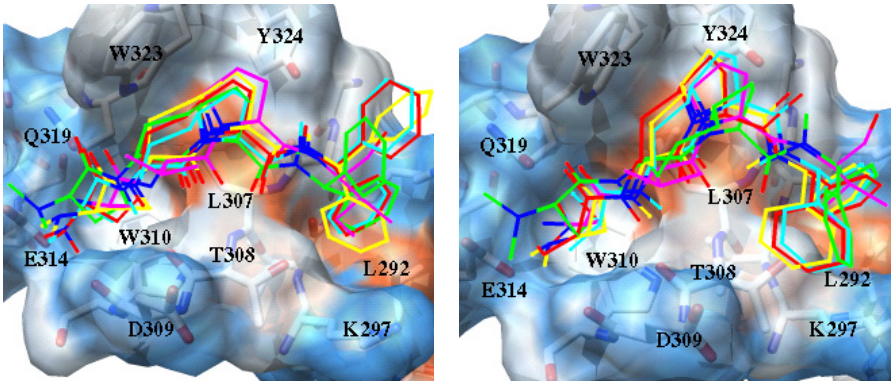

(a) (b)

Fig. 4. The superimpositions of four bicyclic core Smac mimetics and AVPI on the hydrophobic surface of XIAP-BIR3 domain. SM1, SM2, SM3, SM4, and AVPI are shown in red, yellow, green, cyan, and magenta, respectively. (a) the extended conformations; and (b) the bended conformations. Color online.

3.2. *MD simulations*

Because the binding energy of SM4 decreases significantly, only the docking conformations of SM1, SM2, and SM3 were used for MD simulations. The time dependences of RMSDs are shown in Fig. 5. The RMSDs of the protein are stable in all simulations, but those of the Smac mimetics are different.

The dynamics results of SM1 are shown in Figs. 5(a) and 5(b). The RMSD of SM1_a is smooth and stabilizes at 2.0 Å after 5 ns. But that of SM1_b keeps at 1.3 Å before 3 ns and increases abruptly to 3.0 Å after 3 ns. We examined the conformations of SM1_b at different time and found that this change was due to the rotation of the terminal diphenylmethyl. Because the extended conformation matches better with the backbone of AVPI, and the binding affinity is stronger.

Figures 5(c) and 5(d) show the results of SM2, in which the RMSD of SM2_a displays obvious fluctuations at the initial 3 ns and finally stabilizes at 1.7 Å, while that of SM2_b achieves equilibrium at 0.5 ns and keeps at 1.7 Å after 4 ns. This further verifies that the extended form is more stable, and the bended one would always tend to convert into the stable conformation.

Figures 5(e) and 5(f) give the results of SM3 in the MD simulations. The RMSD of SM3_a decreases gradually from 1.7 to 1.0 Å at 1 ns, and stabilizes at 1.5 Å after 4 ns. For SM3_b, its RMSD keeps stable at 2.0 Å after 0.5 ns, but suddenly increases to 3.2 Å. We analyzed the structure of SM3_b and found that of SM3_b changed its conformation to extended conformation.

From the time dependences of RMSDs, we can see that the extended conformations are more stable than the bended ones, which would convert to the extended forms during MD simulations. This result is in good agreement with that of experiments.[48,49]

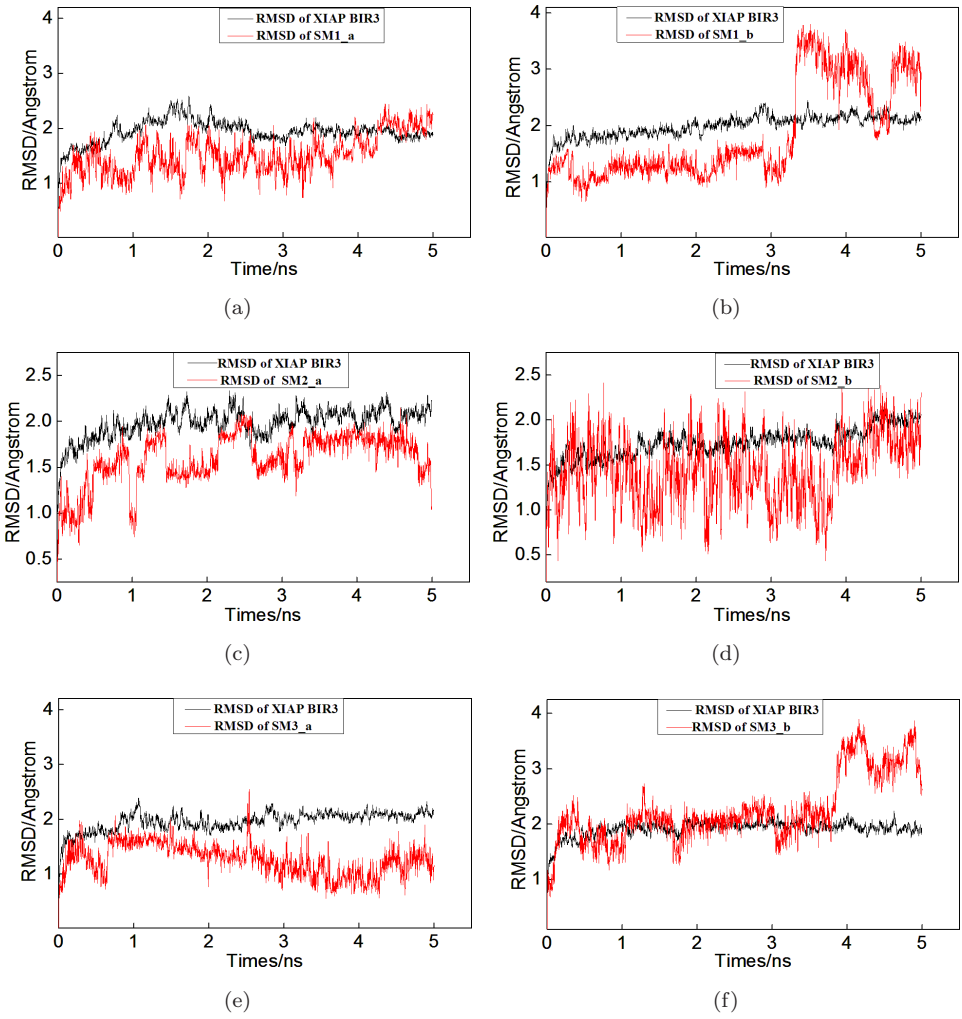

Fig. 5. Time dependence of RMSDs from XIAP-BIR3 domain and three bicyclic core Smac mimetics in 5 ns MD simulations. For each ligand, two different conformations are considered. (a) SM1_a, (b) SM1_b, (c) SM2_a, (d) SM2_b, (e) SM3_a, and (f) SM3_b.

In addition, we examined the distances of some important atoms between Smac mimetics and XIAP-BIR3. Because the hydrogen bonds are mainly distributed among amino-terminus and seven-member rings, we focus our discussions on these two segments, shown in Fig. 6.

Time dependences of distances in the extended and bended conformations of SM1 are given in Figs. 6(a) and 6(b). From the distances of N60_OE1(Glu314) and N60_OE2(Glu314) (labels in Fig. 3), we can see that the hydrogen bonds between the amino-terminus of SM1_a and Glu314 disappear, but the interactions between SM1_a and Thr308 become stronger. Although the hydrogen bond between SM1_b

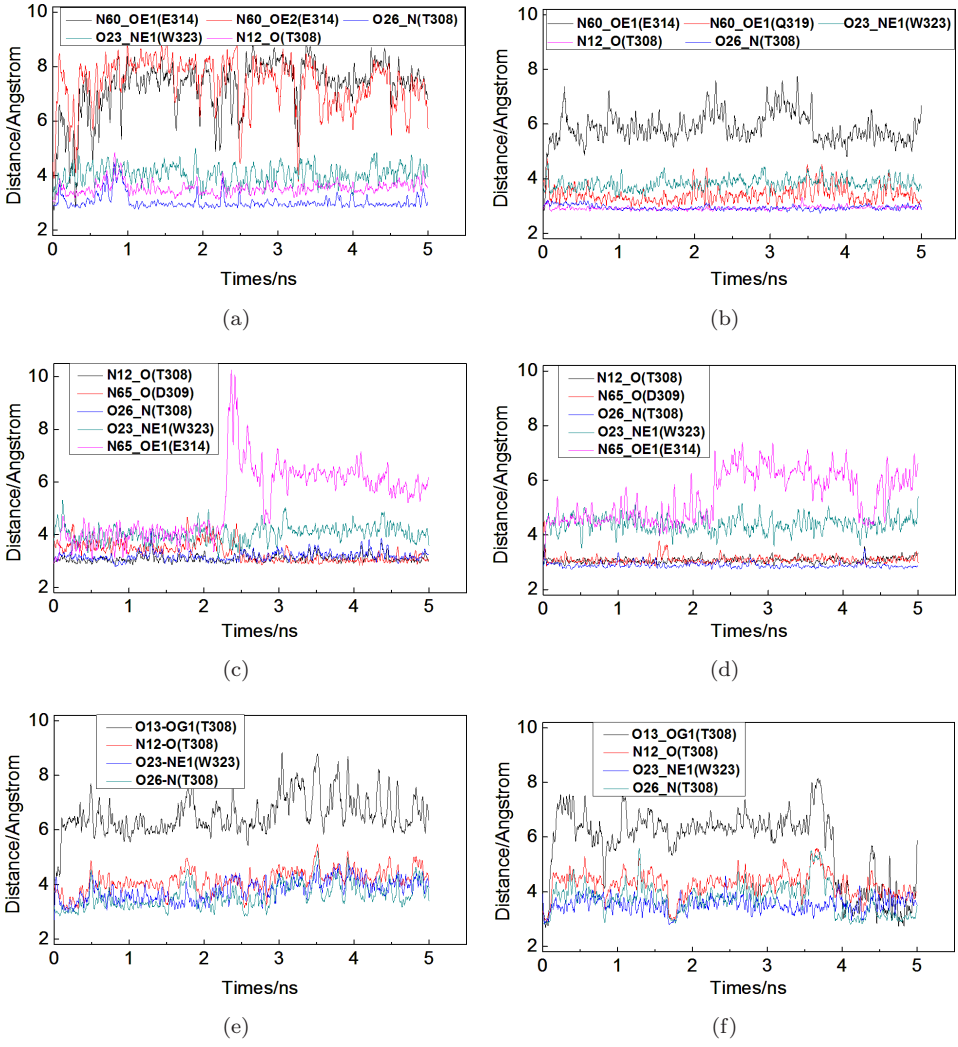

Fig. 6. Time courses of the distances between the important atoms from the Smac mimetics and XIAP-BIR3 domain. The Smac mimetics are (a) SM1_a, (b) SM1_b, (c) SM2_a, (d) SM2_b, (e) SM3_a, and (f) SM3_b.

and Glu314 is abolished (Fig. 6(b)), the one between free amino group and Gln319 is stable. Besides, the distances of N12_O(Thr308) and O26_N(Thr308) indicate that the hydrogen bonding interactions between the seven-member rings and XIAP-BIR3 are stronger in the bended conformations.

The time dependences of the two conformations of SM2 are also given in Figs. 6(c) and 6(d). It can be seen that the interactions between SM2 and Glu314 are suddenly weakened at 2.5 ns in both of the two conformations, while the changes of other distances are similar.

Figures 6(e) and 6(f) show that the distances of both N12_O (Thr308) and O26_N (Thr308) are longer than those in SM1 and SM2, indicating that the interactions between SM3 and XIAP-BIR3 are weakened. The distances of O13_OG1 (Thr308) decrease suddenly at 4 ns, this change is consistent with that of RMSD in Fig. 5(f), suggesting that the terminal diphenylmethyl converts its conformation during the MD simulations.

From the changes of distances in all simulations, we can see that the interactions between the amino group and Glu314 are weakened. But the distances between the seven-member rings of the Smac mimetics and Thr308 are always stable, which suggests that Thr308 makes the stable interactions with Smac mimetics. In other words, Thr308 plays an essential role in stabilizing the complex. We also notice that the distances between SM2 and XIAP-BIR3 are smaller than the other ligands, suggesting a stronger interaction with XIAP-BIR3.

3.3. *Calculation of the binding free energies and energy decomposition*

To accurately calculate the binding free energy of Smac mimetics bound to XIAP-BIR3, and get an insight into the contribution of individual residue to the energy, we used MM_PBSA method to calculate the binding free energy for each complex. The energy terms contributing to the binding free energy by MM_PBSA are shown in Table 2. ΔE_{ELE} and ΔE_{VDW} are electrostatic energy and van der Waals interactions

Table 2. Energy terms contributing to the binding free energy (kcal/mol).

Energy term	SM1_a	SM1_b	SM2_a	SM2_b	SM3_a	SM3_b
ΔE_{ELE}	−27.64	−34.36	−29.82	−26.45	−19.73	−17.45
ΔE_{VDW}	−40.46	−39.63	−42.47	−43.31	−43.25	−40.76
ΔE_{INT}	0.00	0.00	0.00	0.00	0.00	0.00
ΔE_{GAS}	−68.10	−73.98	−72.29	−69.76	−62.98	−58.21
$\Delta G_{\mathrm{PBSUR}}$	−4.96	−4.79	−5.04	−5.10	−5.15	−4.89
$\Delta G_{\mathrm{PBCAL}}$	41.54	50.96	47.95	43.65	42.61	41.91
$\Delta G_{\mathrm{PBSOL}}$	36.59	46.18	42.91	38.55	37.46	37.03
$\Delta G_{\mathrm{PBELE}}$	13.90	16.61	18.13	17.21	22.89	24.47
$\Delta G_{\mathrm{PBTOT}}$	−31.52	−27.81	−29.38	−31.21	−25.51	−21.18
$-T\Delta S_{\mathrm{TOT}}$	22.00	27.19	19.30	24.94	24.51	25.10
$\Delta G_{\mathrm{PB,bind}}$	−9.52	−0.62	−10.08	−6.27	−1.00	3.92
$\Delta G_{(\mathrm{exp}),\mathrm{bind}}$[a]	−10.36		−9.83		−6.60	
$\mathrm{IC}_{50(\mathrm{exp})}/\mu\mathrm{M}$[b]	50		0.1		3.0	

[a]The experimental data are calculated according to RTln(Ki), and the Ki values are from Ref. 31.
[b]The experimental data are from Ref. 31.
Note: ELE is electrostatic energy that is calculated by MM force field, VDW is van der Waals contribution from MM, INT is internal energy from bond, angle, and dihedral terms in the MM force field. GAS = ELE + VDW + INT. PBSUR is the non-polar contribution to the solvation free energy calculated by PB calculations, PBCAL is the electrostatic contribution to the solvation free energy calculated by PB, PBSOL = PBSUR + PBCAL. PBELE = PBCAL + ELE, PBTOT = PBSOL + GAS. ΔS_{TOT} is entropy calculated by normal mode module.

calculated by the MM force field, respectively. ΔE_{INT} (the values are all zero) is the internal energy from bond, angle, and dihedral terms in the MM force field. ΔE_{GAS} is the sum of the above-mentioned three terms. $\Delta G_{\mathrm{PBSUR}}$ and $\Delta G_{\mathrm{PBCAL}}$ account for non-polar and polar contribution to the solvation free energy $\Delta G_{\mathrm{PBSOL}}$ calculated by Poisson–Boltzmann equation. $\Delta G_{\mathrm{PBSOL}}$ is the sum of $\Delta G_{\mathrm{PBSUR}}$ and $\Delta G_{\mathrm{PBCAL}}$ while $\Delta G_{\mathrm{PBELE}}$ is the sum of ΔE_{ELE} and $\Delta G_{\mathrm{PBCAL}}$. ΔS_{TOT} is the conformational entropic changes.[35]

Table 2 shows that the binding free energies ($\Delta G_{\mathrm{PB,bind}}$) of the two conformations for each mimetic are greatly different. For example, the value of SM1_a is −9.65 kcal/mol while that of SM1_b is only −0.62 kcal/mol. From Table 2, one can see that the binding free energies of SM1_a and SM2_a are much closer to the experimental values. These results suggest that these Smac mimetics may adopt extended conformations to bind to XIAP-BIR3. When amino group bears one methyl, the binding free energy is the lowest, but when amino group bearing two methyl groups, the binding free energy decreases a lot.

Figure 7 shows the energy contribution of each residue to the binding energy. It can be seen that 10 residues are mainly responsible for the ligand binding, namely Lys297, Gly306, Leu307, Thr308, Asp309, Trp310, Lys311, Glu314, Gln319, and Trp323, in particular Thr308 contributes a lot.

4. Conclusions

The molecular docking and MD simulations methods were applied to study the binding mode and affinity of four Smac mimetics bound to XIAP-BIR3. The docking results reveal that these Smac mimetics bind to the surface groove, which agrees well with the experimental study. But two competitive conformations were found for each ligand from the docking calculation. The MD simulations show that XIAP-BIR3 is stable during simulations, but for the two conformations of each

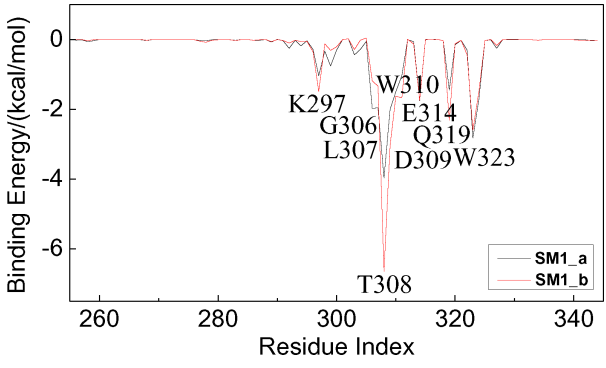

(a)

Fig. 7. Binding energy contribution of each residue of (a) SM1, (b) SM2, and (c) SM3 bound to XIAP-BIR3. The key residues are given in the plots.

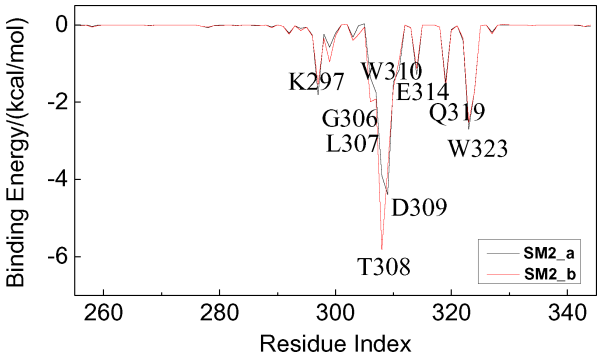

(b)

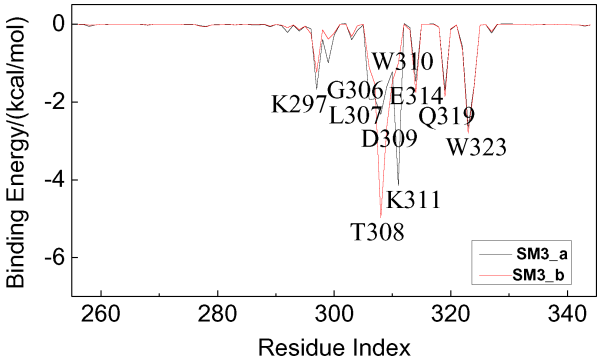

(c)

Fig. 7. (*Continued*)

Smac mimetic, the extended conformation is more stable than the bended one. After MD simulations, the bended conformation would convert to the extended forms. The MM-PBSA calculations reveal that the binding free energy is basically consistent with that of the experiments, and SM2 corresponds to the lowest binding energy. Energy decomposition verifies that residue Thr308 is the biggest contributor to the binding, and Asp309, Glu314, and Trp323 are indispensable for XIAP-BIR3 domain recognizing and binding Smac mimetics.

Acknowledgments

This work is supported by the National Natural Science Foundation of China (20873075) and Natural Science Foundations Shandong Province (ZR2009BM005).

References

1. Hengartner MO, *Curr Opin Genet Dev* **6**:34, 1996.
2. Jacobson MD, Weil M, Raff MC, *Cell* **88**:347, 1997.

3. Hunter AM, LaCasse EC, Korneluk RG, *Apoptosis* **12**:1543, 2007.
4. Riedl SJ, Renatus M, Schwarzenbacher R, Zhou Q, Sun C, Fesik SW, Liddington RC, Salvesen GS, *Cell* **104**:791, 2001.
5. Chai J, Shiozaki E, Srinivasula SM, Wu Q, Dataa P, Alnemri ES, Shi Y, *Cell* **104**: 769, 2001.
6. Srinivasula SM *et al.*, *Nature* **410**:112, 2001.
7. Sun C, Cai M, Meadows RP, Xu N, Gunasekera AH, Herrmann J, Wu JC, Fesik SW, *J Biol Chem* **275**:33777, 2000.
8. Shiozaki EN, Chai J, Rigotti DJ, Riedl SJ, Li P, Srinivasula SM, Alnemri ES, Fairman R, Shi Y, *Mol Cell* **11**:519, 2003.
9. Du C, Fang M, Li Y, Li L, Wang X, *Cell* **102**:33, 2000.
10. Verhagen AM, Ekert PG, Pakusch M, Silke J, Connolly LM, Reid GE, Moritz RL, Simpson RJ, Vaux DL, *Cell* **102**:43, 2000.
11. Shi Y, *Mol Cell* **9**:459, 2002.
12. Shi Y, *Nat Struct Biol* **8**:394, 2001.
13. Sun H, Nikolovska-Coleska Z, Yang C, Qian D, Lu J, Qiu S, Bai L, Peng Y, Cai Q, Wang S, *Account Chem Res* **41**:1264, 2008.
14. Chai J, Du C, Wu J, Kyin S, Wang X, Shi Y, *Nature* **406**:855, 2000.
15. Liu Z, Sun C, Olejniczak ET, Meadows RP, Betz SF, Oost T, Herrmann J, Wu JC, Fesik SW, *Nature* **408**:1004, 2000.
16. Wu G, Chai J, Suber TL, Wu J, Du C, Wang X, Shi Y, *Nature* **408**:1008, 2000.
17. Sun H *et al.*, *J Am Chem Soc* **129**:15279, 2007.
18. Cossu F *et al.*, *J Mol Biol* **392**:630, 2009.
19. Kipp RA *et al.*, *Biochemistry* **41**:7344, 2002.
20. Wist AD, Gu L, Riedl SJ, Shi Y, McLendon GL, *Bioorg Med Chem* **15**:2935, 2007.
21. Nikolovska-Coleska Z *et al.*, *J Med Chem* **47**:2430, 2004.
22. Zobel K *et al.*, *ACS Chem Biol* **1**:525, 2006.
23. Huang JW *et al.*, *J Med Chem* **51**:7111, 2008.
24. Sun H, Nikolovska-Coleska Z, Yang C, Xu L, Tomita Y, Krajewski K, Roller PP, Wang S, *J Med Chem* **47**:4147, 2004.
25. Zhang B, Nikolovska-Coleska Z, Zhang Y, Bai L, Qiu S, Yang C, Sun H, Wang S, Wu Y, *J Med Chem* **51**:7352, 2008.
26. Peng Y, *et al.*, *J Med Chem* **51**:8158, 2008.
27. Sun H *et al.*, *J Med Chem* **51**:7169, 2008.
28. Sun W, Nikolovska-Coleska Z, Qin D, Sun H, Yang C, Bai L, Qiu S, Wang Y, Ma D, Wang S, *J Med Chem* **52**:593, 2009.
29. Sun H *et al.*, *J Am Chem Soc* **126**:16686, 2004.
30. Oost TK *et al.*, *J Med Chem* **47**:4417, 2004.
31. Sun H, Nikolovska-Coleska Z, Lu J, Qiu S, Yang C, Gao W, Meagher J, Stuckey J, Wang S, *J Med Chem* **49**:7916, 2006.
32. Obiol-Pardo C, Granadino-Roldán JM, Rubio-Martinez J, *J Mol Recognit* **21**:190, 2008.
33. Yang C, Sun H, Chen J, Nikolovska-Coleska Z, Wang S, *J Am Chem Soc* **131**:13709, 2009.
34. Kaminski GA, *J Chem Theory Comput* **4**:847, 2008.
35. Obiol-Pardo C, Rubio-Martinez J, *J Chem Inf Model* **47**:134, 2007.
36. Morris GM, Goodsell DS, Halliday RS, Huey R, Hart WE, Belew RK, Olson AJ, *J Comput Chem* **19**:1639, 1998.
37. Frisch MJ *et al.*, *Gaussian 03, Revision C.02*, Gaussian, Inc., Wallingford, CT, 2004.
38. Goodsell DS, Morris GM, Olson AJ, *J Mol Recognit* **9**:1, 1996.

39. Case DA *et al.*, *AMBER 9*, University of California, San Francisco, 2006.
40. Li X, Nevels KJ, Gryczynski Z, Gryczynski I, Pusztai-Carey M, Xie D, Butko P, *Biophys Chem* **144**:53, 2009.
41. Pang Y, *J Mol Model* **5**:196, 1999.
42. Pang Y, *Proteins* **45**:183, 2001.
43. Kollman *et al.*, *Acc Chem Res* **33**:889, 2000.
44. Yam WK, Wahab HA, *J Chem Inf Model* **49**:1558, 2009.
45. Gohlke H, Case DA, *J Comput Chem* **25** 238, 2004.
46. Hu JP, Gong XQ, Su JG, Chen WZ, Wang CX, *Biophys Chem* **132**:69, 2008.
47. Obiol-Pardo C, Rubio-Martinez J, *J Chem Inf Model* **47**:134, 2007.
48. Mastrangelo E *et al.*, *J Mol Biol* **384**:673, 2008.
49. Cossu F *et al.*, *Biochem Biophy Res Commun* **378**:162, 2009.